Mevlana Tıp Bilimleri Dergisi
Mevlana Medical Sciences
eISSN:2757-976X

ARAŞTIRMA MAKALESİ/RESEARCH ARTICLE

DOI:http:/dx.doi.org/10.56752/Mevmedsci.2026.108
Mev Med Sci, 2026; 6(2): 53-61

# Evaluation of Choroidal Vascular Index and Optical Coherence Tomography Angiography Findings in Amblyopic Patients

# Ambliyopik Hastalarda Koroid Vasküler İndeksin ve Optik Koherens Tomografi Anjiyografi Bulgularının Değerlendirilmesi

**Rasit Dilek[1], Abdullah Beyoglu[2], Hamza Kose[3]**

[1]Konya City Hospital, Department of Ophthalmology, Konya, Türkiye
[2]Selçuk University, Medicine Faculty, Department of Ophthalmology, Konya, Türkiye
[3]Abdülkadir Yüksel Hospital, Department of Ophthalmology, Gaziantep, Türkiye

**Makale Tarihleri/Article Dates:**
**Geliş Tarihi/Received:** 3 January 2026
**Kabul Tarihi/Accepted:** 22 April 2026
**Yayın Tarihi/Published Online:** 4 August 2026

**Sorumlu Yazar/Corresponding Author:**
Rasit Dilek,
Konya City Hospital, Konya, Türkiye
**e mail:** r.dilek@hotmail.com

**Açıklama/Disclosure:** Yazarların hiçbiri, bu makalede bahsedilen herhangi bir ürün, aygıt veya ilaç ile ilgili maddi çıkar ilişkisine sahip değildir. Araştırma, herhangi bir dış organizasyon tarafından desteklenmedi. Yazarlar çalışmanın birincil verilerine tam erişim izni vermek ve derginin talep ettiği takdirde verileri incelemesine izin vermeyi kabul etmektedirler.

## ÖZET

**Amaç:** Hipermetropik anizometropik ambliyopili çocuklarda koroid vasküler indeksi (KVİ) ve optik koherens tomografi anjiyografi (OKTA) parametrelerini yaş-cinsiyet eşleştirilmiş sağlıklı gözlerle karşılaştırmak.
**Yöntemler:** Çalışmaya hipermetropik anizometropik ambliyopili 40 çocuk ve 40 sağlıklı kontrol dahil edildi. En iyi düzeltilmiş görme keskinliği, aksiyal uzunluk, merkezi makula kalınlığı, retinal sinir lifi tabakası kalınlığı (RSLT), subfoveal koroid kalınlığı (SFKK), yüzeyel ve derin vasküler dansite (VD), foveal avasküler zon (FAZ) ve KVİ ölçüldü.
**Bulgular:** Aksiyal uzunluk ambliyopik gözlerde sağlıklı ve kontrol gözlerine kıyasla anlamlı kısaydı ($p < 0,001$). SFKK, RSLT, merkezi makula kalınlığı ile lüminal ve stromal alanlarda gruplar arasında anlamlı fark saptanmadı. KVİ ambliyopik gözlerde belirgin düşüktü (sağlıklı göze karşı $p = 0,012$; kontrol gözüne karşı $p = 0,024$). Yüzeyel VD ambliyopik gözlerde azalırken (her iki karşılaştırma için $p = 0,001$) derin VD ve FAZ gruplar arasında farklılık göstermedi.
**Sonuç:** Hipermetropik anizometropik ambliyopi, yüzeyel retinal VD ve koroidal vasküler-stromal dengede seçici değişikliklerle ilişkiliyken derin retinal yapı ve FAZ korunmaktadır. KVİ, ambliyopide koroidal tutulumu değerlendirmek için umut vadeden bir biyobelirteçtir.

**Anahtar Kelimeler:** Ambliyopi, Koroidal Vasküler İndeks, Optik Koherens Tomografi Anjiyografi, Retinal Vasküler Dansite

## ABSTRACT

**Purpose:** To investigate choroidal vascular index (CVI) and optical coherence tomography angiography (OCTA) parameters in children with hyperopic anisometropic amblyopia compared with age- and sex-matched healthy controls.
**Methods:** Forty children with hyperopic anisometropic amblyopia and 40 healthy controls were enrolled. Best-corrected visual acuity, axial length, central macular thickness, retinal nerve fiber layer thickness, subfoveal choroidal thickness, superficial and deep vessel density, foveal avascular zone, and CVI were measured.
**Results:** Axial length was significantly shorter in amblyopic eyes than in fellow and control eyes ($p < 0.001$). Subfoveal choroidal thickness, retinal nerve fiber layer thickness, central macular thickness, and luminal and stromal areas did not differ significantly. CVI was significantly lower in amblyopic eyes (fellow eye: $p = 0.012$; control eye: $p = 0.024$). Superficial vessel density was reduced in amblyopic eyes ($p = 0.001$), while deep vessel density and foveal avascular zone remained comparable.
**Conclusions:** Hyperopic anisometropic amblyopia is associated with selective reductions in superficial vessel density and choroidal vascular-stromal balance, while deep retinal vasculature and foveal avascular zone remain preserved. CVI represents a promising biomarker for evaluating choroidal involvement in amblyopia.

**Key words:** Amblyopia, Choroidal Vascular Index, Optical Coherence Tomography Angiography, Retinal Vessel Density

**Atıf yapmak için/ Cite this article as:** Dilek R, Beyoğlu A, Kose H. Evaluation of Choroidal Vascular Index and Optical Coherence Tomography Angiography Findings in Amblyopic Patients. Mev Med Sci. 2026; 6(2): 53-61

## INTRODUCTION

Amblyopia is a visual disorder that arises as a result of disrupted normal development of binocular vision or insufficient visual stimulation and is clinically defined by a reduction in best-corrected visual acuity (BCVA) in one or both eyes (1). The estimated global prevalence of amblyopia has been reported as 1.36% in a systematic review that included 97 studies conducted in pediatric populations (2). Amblyopia is regarded as one of the leading causes of visual impairment, particularly unilateral vision loss, in children, and constitutes a neurodevelopmental visual disorder that develops as a result of insufficient visual stimulation or abnormal binocular interaction during early childhood; early diagnosis and the timely implementation of appropriate treatments (e.g., occlusion therapy and optical correction) can largely prevent long-term visual impairment, as cases treated at an early age show significant improvements in BCVA (3).

When the etiology of amblyopia is examined in the literature, the two most common subtypes are strabismus-related amblyopia (strabismic amblyopia) and amblyopia secondary to interocular differences in refractive error (anisometropic amblyopia), both of which are considered major causes of the condition. Strabismic and anisometropic mechanisms may lead to amblyopia through distinct neurodevelopmental processes, and each may contribute to amblyopia development either independently or in combination; therefore, amblyopia may arise from strabismus, anisometropia, or a coexistence of both factors (4).

Pioneering studies on the development of the visual pathways began with the experimental work of Hubel and Wiesel, who demonstrated the effects of disrupted binocularly balanced vision on cortical plasticity using models of monocular deprivation and iatrogenic exotropia in animal subjects; these studies revealed that abnormal visual experience during the critical period leads to reversible structural changes in the visual cortex (5). Within the visual system, magnocellular (Y) ganglion cells, which are associated with motion and depth perception, and parvocellular (X) ganglion cells, which are related to color and form perception, project from the retina to the lateral geniculate nucleus via distinct pathways. The function of X cells is critical for high visual acuity; in amblyopic eyes, a reduction in X-cell function has been observed as a consequence of patterned visual deprivation during the critical period (6). At the cortical level, the visual cortex is organized into ocular dominance columns and orientation columns, and the accurate and synchronous representation of inputs from both eyes is essential for normal binocular development; abnormal binocular interactions (e.g., suppression, diplopia, or visual confusion) disrupt binocular integration through cortical inhibitory mechanisms, thereby contributing to the pathogenesis of amblyopia (7, 8). During this critically sensitive period (particularly the first few years of life and ages 6-12), a lack or disruption of appropriate visual stimuli can lead to the development of amblyopia, and early intervention is more effective during this period when visual plasticity is high (5).

The choroid, which plays important roles in eye physiology and homeostasis (such as temperature control, nutrition, and waste removal), may also play a role in the pathophysiology of amblyopia. It is believed that the choroid's ability to change in thickness and volume influences the formation of a clear retinal image (9). Recent studies have demonstrated that changes in subfoveal choroidal thickness (SFCT), which may help regulate the clarity of the retinal image, can occur even over short time periods (10). Studies in the literature have reported that, in amblyopic eyes, both SFCT and macular thickness are greater compared with the fellow eyes of the same patients as well as with the eyes of subjects in the control group (11, 12). However, the analysis of choroidal changes based solely on SFCT may have certain limitations, as SFCT can be influenced by various factors, including age, sex, refractive status, systolic blood pressure, axial length, anterior chamber depth, and lens thickness (13). In addition, diurnal fluctuations in SFCT of up to approximately 20–30 μm have been reported (14). For these reasons, analyses of choroidal changes based on SFCT have been reported to have low repeatability and limited reliability (14). More recently, the binarization technique has enabled the assessment of the choroidal vascular index (CVI), a parameter that integrates both the structural and vascular components of the choroid. CVI has been reported to overcome some of the limitations of choroidal thickness measurements, which may be influenced by systemic and ocular factors such as age and axial length (15).

Optical coherence tomography angiography (OCTA) is a novel, noninvasive vascular imaging technology that enables three-dimensional visualization of retinal blood flow, provides clear delineation of vascular architecture, and allows for layer-by-layer quantitative analysis of retinal perfusion. It has been widely used in the diagnosis and follow-up of various fundus diseases as well as in investigations of disease pathogenesis. Previous OCTA studies have demonstrated reduced vessel density (VD), particularly in the superficial capillary plexus, in amblyopic eyes compared with fellow and control eyes (16-18). In addition, the foveal avascular zone (FAZ), an indicator of foveal development and microvascular integrity, has been evaluated in amblyopia, although results remain inconsistent (16-19). Therefore, OCTA may provide valuable insights into microvascular changes that cannot be detected by conventional structural OCT alone. In this study, we aimed to investigate alterations in the CVI and OCTA findings in patients with amblyopia.

## MATERIALS AND METHODS

A total of 40 anisometropic hyperopic patients aged between 9 and 18 years who received amblyopia treatment at our clinic between January 1, 2017, and March 31, 2018, were retrospectively identified and included by reviewing medical records. In addition, 40 age- and sex-matched healthy subjects were enrolled as a control group. The study included the right eyes of all patients.

Amblyopia was diagnosed as a best-corrected visual acuity (BCVA) of less than 8/10 in one eye with a difference of at least two Snellen lines compared with the fellow eye, which had a BCVA of ≥0.8. Patients were categorized according to the etiology of amblyopia. The refractive amblyopia group included only patients with hyperopic refractive errors and anisometropia defined as an interocular refractive difference of ± 2.0 diopters or greater. Patients with meridional amblyopia or astigmatic amblyopia were excluded. Additionally, patients with amblyopia due to organic causes, a history of ocular surgery, autoimmune or inflammatory diseases that could affect retinal or choroidal involvement or thickness, current medication use, high caffeine consumption or heavy smoking, systemic comorbidities, or poor compliance with OCT imaging were excluded from the study.

The control group consisted of individuals who presented for routine outpatient visits, had no significant refractive error (± 2 Dioptri) or manifest strabismus, demonstrated BCVA of 20/20 in both eyes, and were able to undergo OCT examinations. To ensure data homogeneity, only right eyes were included in the analysis. For all participants, data retrieved from medical records included best-corrected visual acuity measured using a Snellen chart, intraocular pressure measured with a non-contact tonometer (NCT-10, Shin-Nippon, Japan), autorefraction (Tonoref II, Nidek, Japan), slit-lamp biomicroscopy, fundus examination, as well as OCT and OCTA measurements.

All OCT measurements were performed using the same spectral-domain OCT device (ZEISS CIRRUS HD-OCT 5000, Carl Zeiss Meditec, Inc., Dublin, USA). This system operates at an A-scan rate of 27,000 scans per second, utilizes a light source with a central wavelength of 840 nm, and incorporates a superluminescent diode with a bandwidth of 85 nm. It provides an axial tissue resolution of approximately 5 μm and a scanning depth of 2 mm. The device scans a 6 × 6 mm area for both macular and optic disc imaging. For the Optic Disc Cube protocol, 200 B-scans consisting of 200 A-scans each were acquired, while the Macular Cube protocol comprised 128 B-scans with 512 A-scans per B-scan. (20) Retinal nerve fiber layer (RNFL) thickness was measured using the standard 200 × 200 optic disc cube scan protocol with the eye-tracking system activated, by scanning a peripapillary circular area with an approximate diameter of 3.46 mm. The analysis provided global and sectoral RNFL thickness values, including the temporal, superotemporal, superonasal, nasal, inferonasal, and inferotemporal sectors, and the global measurement was accepted as the mean RNFL thickness. Central macular thickness was obtained from the macular thickness map analysis generated by the SD-OCT system.

For choroidal imaging, a high-resolution 21-line enhanced depth imaging (EDI) foveal scan was obtained from each participant. Images with poor signal strength, focal signal loss, or motion artifacts were excluded from the analysis. Subfoveal choroidal thickness was defined as the distance between the outer border of the hyperreflective retinal pigment epithelium and the inner surface of the sclera, and was manually measured at the fovea by the same experienced, independent, masked observer using the device's built-in software (21). Each measurement was repeated twice, and the mean of the two measurements was used for the final analysis. All OCT examinations were performed between 08:00 and 12:00 to minimize the effects of diurnal variation, and participants were instructed to abstain from coffee, smoking, chocolate, and fluid intake for at least three hours prior to the measurements.

The choroidal stromal area and choroidal luminal area were evaluated using the method described by Sonoda et al. (22) Briefly, in EDI–SD-OCT images, the upper boundary of the region of interest (ROI) was defined as the retinal pigment epithelium (RPE) line, and the lower boundary as the choroidoscleral interface. The analyzed area was selected as a 1,500 μm–wide region centered on the fovea, extending 750 μm nasally and 750 μm temporally. Binarization of the choroidal area on OCT images was performed using ImageJ software (version 1.53; National Institutes of Health, USA; http://imagej.nih.gov/ij/). After defining the ROI, three choroidal vessels with luminal areas larger than 100 μm² were randomly selected, and their mean luminal reflectivity was measured. After setting the mean brightness value as the minimum threshold, the image was converted to 8-bit format and binarized using Niblack's auto local thresholding method (23). The binarized image was then reconverted to an RGB (red, green, blue) format, and the luminal area was identified using the threshold tool. After incorporating the distance calibration data for each pixel, the total choroidal area, luminal area, and stromal area were automatically calculated. Light pixels were defined as the choroidal stromal area, whereas dark pixels were defined as the choroidal luminal area. The CVI was calculated as the ratio of the luminal area to the total choroidal area (Figure 1).

High-quality images of the retinal structure and vessel network were obtained using spectral domain OCTA, RTVue-XR AngioVue (software version: 2015.1.0.90; Optovue Inc.,

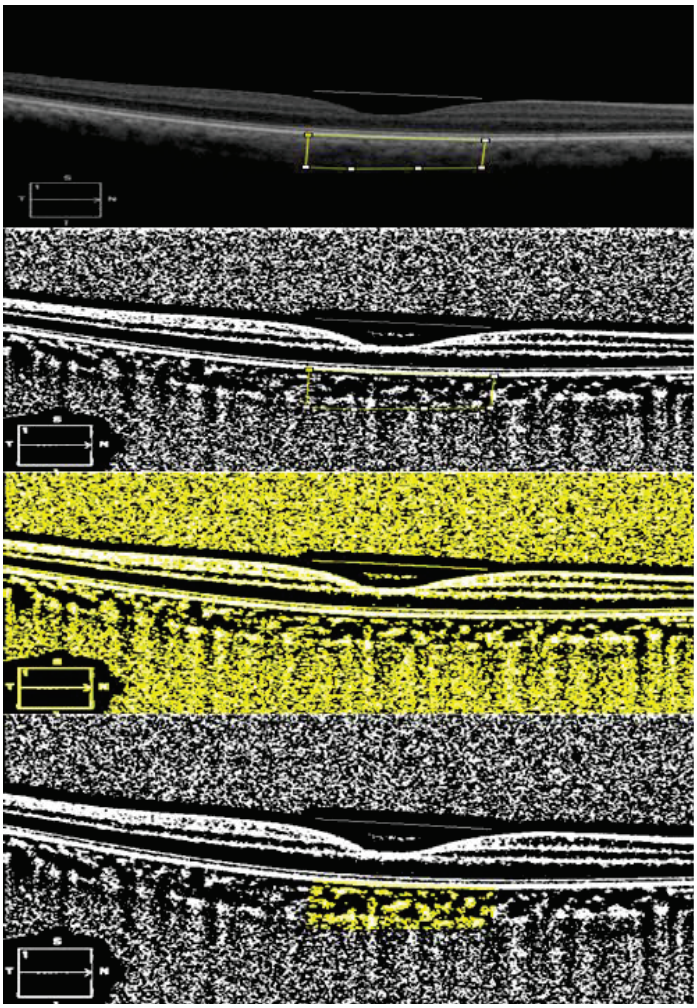

**Figure 1.** Calculation of choroidal vascular index with Image J program; determining the area to be calculated, applying Niblack's auto local threshold and determining the regions representing the lumen area using the color threshold tool.

Fremont, CA, USA). The XR Avanti AngioVue spectral domain OCTA (software version 2015.1.1.98, Optovue Inc., Fremont, CA) is a device which obtains volumetric scans of 304 pixels × 304 pixels A-scans at 70,000 A-scans per second, using a light source of 840 nm and an axial resolution of 5 µm. The Optovue AngioVue system technology provides quantitative analysis and numerical data about vascular density (VD) and flow area. The OCTA system, which uses blood flow as intrinsic contrast, is based on the split-spectrum amplitude-decorrelation angiography (SSADA) algorithm. Using 5 repeated B-scans at 216 raster positions, three-dimensional (3D) OCTA scans were obtained over regions 6 × 6 mm in size. Each B-scan was formed of 216 A-scans, with 304 pixels × 304 pixels in the transverse dimension. The B-scan frame rate was 270 frames per second, and thus each scan was obtained in approximately 3.0 s (24).

The OCTA images were obtained using an RTVueXR Avanti machine (AngioVue; Optovue Inc., Fremont, CA). The integral SSADA algorithm and motion correlation technology of the AngioVue system were both used. Discrimination of the superficial capillary plexus (SCP), deep capillary plexus (DCP) outer retina and choroidal capillary layers was provided by the automatic segmentation of the intraretinal layers. The segmentation of the SCP on the OCTA image was applied with the placement of an inner boundary 3 µm below the internal limiting membrane and an outer boundary 16 µm below the inner plexiform layer and the DCP 16 mm to 70 µm below the inner plexiform layer. The outer retina is defined as 70 µm below the inner plexiform layer and 30 µm below the retinal pigment epithelium. Angiographic analysis was made using a 6 x 6 mm frame which allowed the evaluation of the perifoveal region, the foveal avascular zone (FAZ) and the parafoveal region (25, 26).

VD was calculated as the percentage of the selected region covered by vessels and microvessels. The mean VD was automatically calculated by the software in both the SCP and DCP. Avascular region (larger than the normal gap between capillaries) is a significant area displaying lack of flow signal on en face angiogram. The FAZ was used as an anatomical landmark to locate the retinal point of fixation and was measured on SCP and DCP (Figure 2).

***Statistical Analysis***

All statistical analyses were performed using SPSS software (SPSS Inc., version 14.01). Descriptive statistics were calculated, with continuous variables expressed as mean ± standard deviation and categorical variables presented as percentages. The chi-square test was used for comparisons of categorical variables. Prior to inferential analyses, the distribution of all continuous variables was assessed for normality using the Kolmogorov–Smirnov test. Differences between the study and control groups for continuous variables were evaluated using the Student's t-test for normally distributed data and the Mann–Whitney U test for non-normally distributed data. A P value of less than 0.05 was considered statistically significant. Intraobserver reliability for subfoveal choroidal thickness, luminal area, stromal area, and total choroidal area measurements was assessed using the intraclass correlation coefficient (ICC).

## RESULTS

A total of 22 male and 18 girl patients with anisometropic amblyopia were included in the study, along with an equal number of age- and sex-matched healthy controls. The mean age of the patient group was 11.25 ± 2.15 years, while the mean age of the control group was 11.98 ± 2.58 years, with no statistically significant difference between the patient and

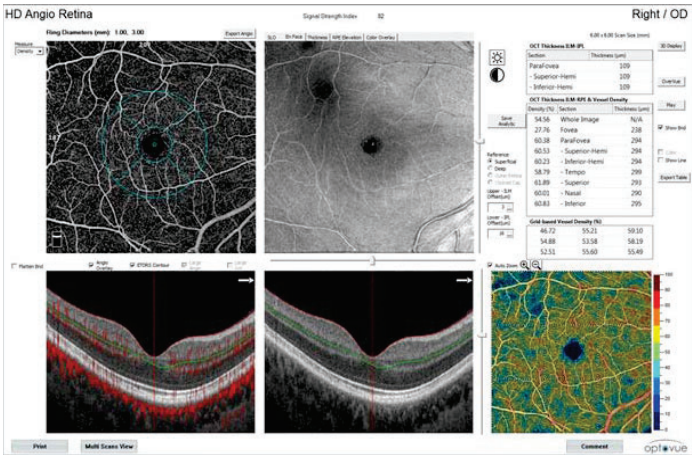


**Figure 2a.** Image demonstrating VD in a non-amblyopic eye at the level of the SCP. VD was automatically calculated, with a mean value of 54.56%.
**Abbreviations:** SCP, superficial capillary plexus; VD, vessel density.

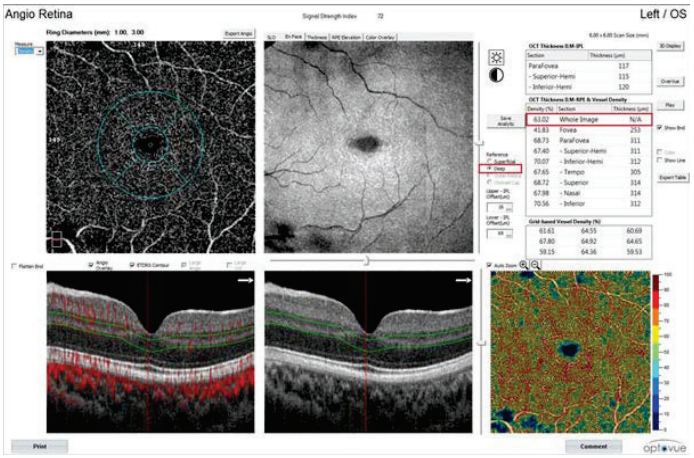


**Figure 2b.** Image demonstrating vessel density in a non-amblyopic eye at the level of the DCP. VD was automatically calculated, with a mean value of 63.02%.
**Abbreviations:** DCP, deep capillary plexus; VD, vessel density.

**Table 1.** Comparison of age, best-corrected visual acuity, axial length, autorefraction (diopters), and intraocular pressure between the patient and control groups.

| Parameter | Amblyopic Eye (n=40) | Fellow Eye (n=40) | Control Group (n=40) | P value* |
|---|---|---|---|---|
| Age (years) | 11.25 ± 2.15 | 11.25 ± 2.15 | 11.98 ± 2.58 | 0.789 |
| BCVA (letters) | 0.36 ± 0.25 | 0.96 ± 0.11 | 0.95 ± 0.12 | <0.001, <0.001 |
| Axial Length (mm) | 20.97 ± 3.18 | 22.12 ± 2.85 | 22.98 ± 3.27 | <0.001, <0.001 |
| Autorefraction (D) | +5.12 ± 2.58 | +1.28 ± 2.15 | +0.55 ± 2.29 | <0.001, <0.001 |
| Intraocular Pressure (mmHg) | 16.52 ± 2.75 | 15.93 ± 3.12 | 16.78 ± 3.93 | 0.925, 0.689 |

Note: mm = millimeters; mmHg = millimeters of mercury.
* The first P value indicates the comparison between amblyopic and fellow eyes; the second P value indicates the comparison between amblyopic eyes and the control group.

**Table 2.** Comparison of retinal and choroidal parameters between amblyopic eyes, fellow eyes, and control eyes.

| Parameter | Amblyopic Eye (n=40) | Fellow Eye (n=40) | Control Group (n=40) | P value* |
|---|---|---|---|---|
| Central Macular Thickness (μm) | 238.85 ± 22.65 | 241.27 ± 28.52 | 244.32 ± 31.12 | 0.420, 0.568 |
| Retinal Nerve Fiber Layer (RNFL) Thickness (μm) | 96.5 ± 8.9 | 97.1 ± 10.5 | 98.5 ± 9.0 | 0.231, 0.189 |
| Subfoveal Choroidal Thickness (μm) | 365.12 ± 38.1 | 351.25 ± 41.2 | 342.8 ± 34.0 | 0.739, 0.296 |
| Luminal Area (pixels) | 769,124.4 ± 112,314.8 | 742,885.8 ± 99,564.2 | 726,998.0 ± 102,748.8 | 0.129, 0.085 |
| Stromal Area (pixels) | 335,811.1 ± 58,121.8 | 325,862.4 ± 47,723.2 | 316,763.3 ± 48,429.1 | 0.562, 0.285 |
| Total Choroidal Area (pixels) | 1,152,214.8 ± 125,889.2 | 1,058,987.7 ± 122,451.9 | 1,046,968.8 ± 114,237.3 | 0.120, 0.095 |
| Choroidal Vascular Index (CVI) | 0.669 ± 0.09 | 0.691 ± 0.17 | 0.690 ± 0.24 | 0.012, 0.024 |

Note: μm = micrometers. *The first P value indicates the comparison between amblyopic and fellow eyes; the second P value indicates the comparison between amblyopic eyes and the control group.

control groups (p = 0.789). The BCVA of the amblyopic eyes was 0.36 ± 0.25, compared with 0.96 ± 0.11 in the fellow eyes and 0.95 ± 0.12 in the control group (p <0.001). The mean axial length was 20.97 ± 3.18 mm in amblyopic eyes, 22.12 ± 2.85 mm in fellow eyes, and 22.98 ± 3.27 mm in the control group (p <0.001). The mean autorefractive value was +5.12 ±

**Table 3.** Comparison of OCTA parameters between amblyopic eyes, fellow eyes, and control eyes.

| Parameter | Amblyopic Eye (n=40) | Fellow Eye (n=40) | Control Group (n=40) | P value* |
|---|---|---|---|---|
| Superficial Vessel Density (VD, %) | 49.78 ± 3.24 | 54.99 ± 3.01 | 55.14 ± 2.89 | 0.001, 0.001 |
| Deep Vessel Density (VD, %) | 44.12 ± 3.51 | 45.12 ± 2.89 | 45.99 ± 3.12 | 0.621, 0.489 |
| Superficial FAZ Area ($mm^2$) | 0.30 ± 0.12 | 0.32 ± 0.14 | 0.31 ± 0.12 | 0.425, 0.352 |
| Deep FAZ Area ($mm^2$) | 0.33 ± 0.13 | 0.34 ± 0.14 | 0.35 ± 0.09 | 0.628, 0.192 |

Note: VD = vessel density; FAZ = foveal avascular zone; $mm^2$ = square millimeters. *The first P value indicates the comparison between amblyopic and fellow eyes; the second P value indicates the comparison between amblyopic eyes and the control group.

2.58 D in amblyopic eyes, +1.28 ± 2.15 D in fellow eyes, and +0.55 ± 2.29 D in the control group (p <0.001). These findings are summarized in Table 1.

Retinal and choroidal parameters in the patient and healthy groups are presented in Table 2. Accordingly, no statistically significant differences were observed in central macular thickness (CMT), RNFL thickness, or SFCT when amblyopic eyes were compared with either the fellow eyes or the control group. In contrast, the CVI was significantly reduced in amblyopic eyes compared with both the fellow eyes and the control group (p =0.012 and p=0.024, respectively). OCTA data are presented in Table 3. In SCP measurements, a statistically significant reduction was observed in amblyopic eyes compared with both the fellow eyes and the control group (p =0.001 vs fellow eyes and p = 0.001 vs controls). However, no statistically significant differences were detected in deep vascular density measurements between amblyopic eyes and either the fellow eyes or the control group (p=0.621 and p=0.489, respectively).

No statistically significant differences were found in superficial or deep FAZ measurements when amblyopic eyes were compared with the fellow eyes (p=0.425 and p=0.628, respectively) or with the control group (p=0.352 and p=0.192, respectively).

## DISCUSSION

Although the etiology of amblyopia has not yet been fully elucidated, several neuroanatomical and functional mechanisms have been proposed to explain its pathophysiology. Classical experimental and clinical studies have demonstrated that abnormal visual experience during the critical period leads to lasting structural and functional alterations in the lateral geniculate nucleus and the visual cortex; as a consequence, reductions in synaptic connectivity and disruptions in cortical projections may occur (27). However, in recent years, it has been increasingly recognized that amblyopia is not solely a cortical disorder; subcortical structures and ocular tissues—particularly the choroid—may also be involved in this process. Advances in OCT technologies, particularly EDI-OCT and swept-source OCT, have enabled detailed in vivo assessment of the structural and vascular characteristics of the choroid (28, 29). Numerous studies in the literature have reported increased SFCT in amblyopic eyes compared with fellow or control eyes. This increase has been shown to be particularly pronounced in cases of anisometropic and hyperopic amblyopia (30). This finding has been suggested to be associated with delayed emmetropization or alterations in choroidal hemodynamics. However, the fact that SFCT is affected by numerous factors such as age, axial length, refractive status, and diurnal variation limits the use of this parameter alone as a reliable biomarker (28).

The CVI reflects the proportion of the luminal area within the total choroidal area and is considered a more stable and physiologically meaningful parameter than SFCT for evaluating the vascular–stromal balance of the choroid. In the present study, CVI values were found to be significantly reduced in cases of hyperopic anisometropic amblyopia; in contrast, no statistically significant difference was observed in the luminal area representing choroidal vessels. This finding suggests that, rather than an absolute vascular loss, a disproportionate increase in the stromal component may be present in amblyopia. Recent studies similarly propose that stromal tissue expansion may occur in amblyopic eyes and that this phenomenon could be related to chronic low-grade inflammation, extracellular matrix remodeling, or impaired vascular maturation (30-33). On the other hand, there are also studies in the literature reporting differences in subfoveal choroidal thickness and total choroidal area between amblyopic and control eyes, despite finding no significant differences in CVI between the groups (30-32). In a study evaluating choroidal structure in hyperopic amblyopic eyes, CVI was reported to be higher in amblyopic eyes compared with fellow eyes and to show a positive correlation with SFCT (33). In contrast, another study reported that CVI was significantly lower in eyes with hyperopic anisometropic amblyopia compared with both fellow eyes and healthy controls (30). These conflicting results may be explained by factors such as heterogeneity among amblyopia subtypes, differences in refractive error distribution, variations in axial length, age-related differences, and the binarization methods used for OCT image analysis. Indeed, some studies focusing on anisometropic amblyopia have reported that total choroidal area and luminal area correlate with refractive

error and axial length, whereas CVI remains relatively stable; this finding has been interpreted as indicating that CVI may better reflect intrinsic vascular alterations independent of ocular geometry (31). Recent three-dimensional analyses using swept-source OCTA have demonstrated alterations in parameters such as choroidal vascular volume and volumetric CVI in amblyopic eyes. These findings indicate that choroidal changes in amblyopia are not limited to increases or decreases in thickness alone but may be associated with spatial reorganization of the vascular network (34, 35).

Most studies investigating the use of OCTA in children with anisometropic and strabismic amblyopia have found no significant difference in FAZ area between amblyopic eyes and normal control eyes (16-19, 36), this finding is consistent with our results. Accordingly, the findings of the present study suggest that the retinal vascular architecture is largely preserved in children with amblyopia. Several studies in the literature have reported that vessel density in the SCP is lower in amblyopic eyes compared with healthy eyes and age-matched control groups (16, 17). Cheung and colleagues suggested that the observed reduction in blood flow density may be associated with shorter axial length in healthy children and could, in part, result from measurement magnification errors (37). In contrast, some studies have found no significant correlation between axial length or refractive power and retinal vascular parameters (18).

In our study, superficial VD was found to be significantly reduced, whereas no significant differences were observed in the DCP or FAZ measurements. These findings are consistent with studies reporting selective involvement of the SCP (38, 39). It has been reported that measurements of the deep capillary plexus may be affected by projection artifacts originating from the superficial layer, leading to potential measurement errors; additionally, high interobserver variability has been described for FAZ measurements obtained using the same device (37, 40). This highlights the need for caution when interpreting findings related to the DCP. Moreover, comparisons based on amblyopia subtypes have yielded conflicting results in the literature. No significant differences in RNFL thickness or macular parameters have been reported between strabismic and anisometropic amblyopia groups (41). In contrast, Kee and colleagues reported that the fovea was thicker in children with strabismic amblyopia, whereas the retinal nerve fiber layer was thicker in children with anisometropic amblyopia (42). Yen and colleagues reported that in patients with anisometropia, the RNFL thickness of amblyopic eyes was greater than that of fellow eyes, whereas this finding was not observed in patients with strabismus (43). Similarly, Yoon and colleagues reported that RNFL thickness was significantly greater in hyperopic anisometropic amblyopia (44).

This study has several limitations. First, its retrospective design and relatively small sample size may limit the generalizability of the findings. Second, only hyperopic anisometropic amblyopia was included, and other amblyopia subtypes were not evaluated. Third, measurements were obtained using a single OCTA device, and potential segmentation errors or projection artifacts may have affected the accuracy of vascular parameters. In addition, axial length–related magnification effects were not fully corrected, which may influence OCTA measurements. Finally, the cross-sectional nature of the study precludes assessment of causal relationships and longitudinal changes. In conclusion, our study demonstrates that CVI — a biomarker of choroidal vascular-stromal balance — is significantly reduced in amblyopic eyes with hyperopic anisometropic amblyopia. Although luminal, stromal, and total choroidal areas did not differ significantly between groups, the reduction in CVI suggests that the proportional composition of the choroid may be altered independently of absolute volumetric changes. The numerically higher stromal area observed in amblyopic eyes does not reach statistical significance and therefore cannot be interpreted as a definitive finding; it may, however, represent a trend worthy of investigation in future studies with larger sample sizes. The underlying mechanisms of these changes — including disruption of ocular growth signals from normal visual input, alterations in autonomic mechanical regulation, or plasticity within central visual pathways — remain to be fully elucidated. Prospective studies with broader cohorts, incorporating CVI and volumetric choroidal analyses standardized for age, refractive error, and degree of amblyopia alongside functional visual outcomes, will more clearly define the role of choroidal involvement in the pathophysiology of amblyopia.

**Ethics Committee Approval:** This retrospective observational study was conducted at the Department of Ophthalmology, Sütçü İmam University, in accordance with the principles of the Declaration of Helsinki, and ethical approval was obtained from the local ethics committee (Sütçü İmam University Faculty of Medicine Ethics Committee, Kahramanmaraş, Türkiye; Decision No: 2018/07; Date: April 4, 2018)

**Conflict of interest:** The authors declared no conflicts of interest with respect to the authorship and/or publication of this article.

**Financial conflict of interest:** Authors declares that he did not receive any financial support in this study.

**Address correspondence to:** Rasit Dilek,
Konya City Hospital, Konya, Türkiye
**e-mail:** r.dilek@hotmail.com

**REFERENCES**

1. Tailor V, Bossi M, Greenwood JA, Dahlmann-Noor A. Childhood amblyopia: current management and new trends. British Medical Bulletin. 2016;119(1):75.
2. Hu B, Liu Z, Zhao J, Zeng L, Hao G, Shui D, et al. The global prevalence

of amblyopia in children: a systematic review and meta-analysis. Frontiers in pediatrics. 2022;10:819998.
3. Koçak G, Duranoğlu Y. Ambliyopi ve tedavisi. Turk J Ophthalmol. 2014;44:228-36.
4. Duman R, ATİLLA H. Clinical course and response to therapy in different types of amblyopia Farkli {dotless} ambliyopi tiplerinde klinik seyir ve tedavi. Turk Oftalmoloiji Dergisi. 2013;43(5).
5. JJ K. Şaşılık: Şaşılığın Fonksiyonel Sonuçları. Klinik Oftalmoloji 4th ed İstanbul Nobel Tıp Kitabevleri Ltd Şti. 2001:518-21.
6. Ganong W. Tıbbi Fizyoloji "20. Baskı". Çev Ed Türk Fizyolojik Bilimler Derneği Nobel Tıp Kitabevleri, Ankara. 2001.
7. Grigg J, Thomas R, Billson F. Neuronal basis of amblyopia: a review. Indian journal of ophthalmology. 1996;44(2):69-76.
8. Ikeda H. Visual acuity, its development and amblyopia. Journal of the Royal Society of Medicine. 1980;73(8):546-55.
9. Nickla DL, Wallman J. The multifunctional choroid. Progress in retinal and eye research. 2010;29(2):144-68.
10. Chiang STH, Phillips JR, Backhouse S. Effect of retinal image defocus on the thickness of the human choroid. Ophthalmic and Physiological Optics. 2015;35(4):405-13.
11. Li J, Ji P, Yu M. Meta-analysis of retinal changes in unilateral amblyopia using optical coherence tomography. European journal of ophthalmology. 2015;25(5):400-9.
12. Liu Y, Dong Y, Zhao K. A meta-analysis of choroidal thickness changes in unilateral amblyopia. Journal of ophthalmology. 2017;2017(1):2915261.
13. Wei WB, Xu L, Jonas JB, Shao L, Du KF, Wang S, et al. Subfoveal choroidal thickness: the Beijing eye study. Ophthalmology. 2013;120(1):175-80.
14. Tan CS, Ouyang Y, Ruiz H, Sadda SR. Diurnal variation of choroidal thickness in normal, healthy subjects measured by spectral domain optical coherence tomography. Investigative ophthalmology & visual science. 2012;53(1):261-6.
15. Abdolrahimzadeh S, Di Pippo M, Ciancimino C, Di Staso F, Lotery AJ. Choroidal vascularity index and choroidal thickness: potential biomarkers in retinitis pigmentosa. Eye. 2023;37(9):1766-73.
16. Yilmaz I, Ocak OB, Yilmaz BS, Inal A, Gokyigit B, Taskapili M. Comparison of quantitative measurement of foveal avascular zone and macular vessel density in eyes of children with amblyopia and healthy controls: an optical coherence tomography angiography study. Journal of American Association for Pediatric Ophthalmology and Strabismus. 2017;21(3):224-8.
17. Lonngi M, Velez FG, Tsui I, Davila JP, Rahimi M, Chan C, et al. Spectral-domain optical coherence tomographic angiography in children with amblyopia. JAMA ophthalmology. 2017;135(10):1086-91.
18. Doğuizi S, Yılmazoğlu M, Kızıltoprak H, Şekeroğlu MA, Yılmazbaş P. Quantitative analysis of retinal microcirculation in children with hyperopic anisometropic amblyopia: an optical coherence tomography angiography study. Journal of American Association for Pediatric Ophthalmology and Strabismus. 2019;23(4):201. e1-. e5.
19. Karabulut M, Karabulut S, Sül S, Karalezli A. Microvascular changes in amblyopic eyes detected by optical coherence tomography angiography. Journal of American Association for Pediatric Ophthalmology and Strabismus. 2019;23(3):155. e1-. e4.
20. Brautaset R, Birkeldh U, Frehr Alstig P, Wiken P, Nilsson M. Repeatability using automatic tracing with Canon OCT-HS100 and Zeiss Cirrus HD-OCT 5000. PLoS One. 2016;11(2):e0149138.
21. Yiu G, Pecen P, Sarin N, Chiu SJ, Farsiu S, Mruthyunjaya P, et al. Characterization of the choroid-scleral junction and suprachoroidal layer in healthy individuals on enhanced-depth imaging optical coherence tomography. JAMA ophthalmology. 2014;132(2):174-81.
22. Sonoda S, Sakamoto T, Yamashita T, Uchino E, Kawano H, Yoshihara N, et al. Luminal and stromal areas of choroid determined by binarization method of optical coherence tomographic images. American journal of ophthalmology. 2015;159(6):1123-31. e1.
23. Sonoda S, Sakamoto T, Yamashita T, Shirasawa M, Uchino E, Terasaki H, et al. Choroidal structure in normal eyes and after photodynamic therapy determined by binarization of optical coherence tomographic images. Investigative ophthalmology & visual science. 2014;55(6):3893-9.
24. Karti O, Zengin MO, Kerci SG, Ayhan Z, Kusbeci T. Acute effect of caffeine on macular microcirculation in healthy subjects: an optical coherence tomography angiography study. Retina. 2019;39(5):964-71.
25. Choi W, Mohler KJ, Potsaid B, Lu CD, Liu JJ, Jayaraman V, et al. Choriocapillaris and choroidal microvasculature imaging with ultrahigh speed OCT angiography. PloS one. 2013;8(12):e81499.
26. Jia Y, Wei E, Wang X, Zhang X, Morrison JC, Parikh M, et al. Optical coherence tomography angiography of optic disc perfusion in glaucoma. Ophthalmology. 2014;121(7):1322-32.
27. Daw NW. Critical periods and amblyopia. Archives of ophthalmology. 1998;116(4):502-5.
28. Read SA, Collins MJ, Vincent SJ, Alonso-Caneiro D. Choroidal thickness in childhood. Investigative ophthalmology & visual science. 2013;54(5):3586-93.
29. Vira J, Marchese A, Singh RB, Agarwal A. Swept-source optical coherence tomography imaging of the retinochoroid and beyond. Expert Review of Medical Devices. 2020;17(5):413-26.
30. Furundaoturan O, Değirmenci C, Akkın C, Biler ED, Üretmen Ö, Nalçacı S, et al. Evaluation of choroidal vascular Index in amblyopic patients. Turkish Journal of Ophthalmology. 2022;52(3):168.
31. Köksaldı S, Kayabaşı M, Kefeli I, Engin CD, Öztürk T, Grzybowski A. Choroidal vascular characteristics in anisometropic amblyopia: a comparative analysis. BMC ophthalmology. 2025;25(1):301.
32. Nishi T, Ueda T, Mizusawa Y, Shinomiya K, Semba K, Mitamura Y, et al. Choroidal structure in children with anisohypermetropic amblyopia determined by binarization of optical coherence tomographic images. PLoS One. 2016;11(10):e0164672.
33. Baek J, Lee A, Chu M, Kang NY. Analysis of choroidal vascularity in children with unilateral hyperopic amblyopia. Scientific reports. 2019;9(1):12143.
34. Won J, Yaghy A, Ploner S, Takahashi H, Reimann M, Girgis JM, et al. Motion correction and volume merging of ultrahigh resolution OCT enable 3D visualization and longitudinal tracking of hyperreflective foci. Investigative Ophthalmology & Visual Science. 2023;64(9):PP0018-PP.
35. Cao Y, Zhang Y, Gu X, Zhu D, Yang L. Choroid vascular changes in hyperopic anisometropia amblyopia using SS-OCTA. BMC ophthalmology. 2023;23(1):379.
36. Demirayak B, Vural A, Onur IU, Kaya FS, Yigit FU. Analysis of macular vessel density and foveal avascular zone using spectral-domain optical coherence tomography angiography in children with amblyopia. Journal of Pediatric Ophthalmology & Strabismus. 2019;56(1):55-9.
37. Cheung CY, Li J, Yuan N, Lau GYL, Chan AYF, Lam A, et al. Quantitative retinal microvasculature in children using swept-source optical coherence tomography: the Hong Kong Children Eye Study. British Journal of Ophthalmology. 2019;103(5):672-9.
38. Liu C, Zhang Y, Gu X, Wei P, Zhu D. Optical coherence tomographic angiography in children with anisometropic amblyopia. BMC ophthalmology. 2022;22(1):269.
39. Chen W, Lou J, Thorn F, Wang Y, Mao J, Wang Q, et al. Retinal microvasculature in amblyopic children and the quantitative relationship between retinal perfusion and thickness. Investigative ophthalmology & visual science. 2019;60(4):1185-91.

40. Sacconi R, Borrelli E, Querques G. Reproducibility of vessel density, fractal dimension, and foveal avascular zone using 7 different optical coherence tomography angiography devices. American Journal of Ophthalmology. 2018;192:252-3.
41. Firat PG, Ozsoy E, Demirel S, Cumurcu T, Gunduz A. Evaluation of peripapillary retinal nerve fiber layer, macula and ganglion cell thickness in amblyopia using spectral optical coherence tomography. International Journal of Ophthalmology. 2013;6(1):90.
42. Kee S-Y, Lee S-Y, Lee Y-C. Thicknesses of the fovea and retinal nerve fiber layer in amblyopic and normal eyes in children. Korean journal of ophthalmology. 2006;20(3):177-81.
43. Yen M-Y, Cheng C-Y, Wang A-G. Retinal nerve fiber layer thickness in unilateral amblyopia. Investigative ophthalmology & visual science. 2004;45(7):2224-30.
44. Cohen MJ, Kaliner E, Frenkel S, Kogan M, Miron H, Blumenthal EZ. Morphometric analysis of human peripapillary retinal nerve fiber layer thickness. Investigative ophthalmology & visual science. 2008;49(3):941-4.